Reliability of Tibiofemoral Contact Area and Centroid Location in an Upright, Open MRI (UO-MRI)

Andrew Schmidt (aschmid2@stanford.edu)
Stanford University School of Medicine https://orcid.org/0000-0003-3826-6122
David J. Stockton
The University of British Columbia Department of Orthopaedics, UBC Clinician Investigator Program, Centre for Hip Health and Mobility
Michael A. Hunt
The University of British Columbia Department of Physical Therapy, UBC Motion Analysis and Biofeedback Lab, Centre for Hip Health and Mobility
Andrew Yung
The University of British Columbia MRI Research Center, Centre for Hip Health and Mobility
Bassam A. Masri
University of British Columbia Department of Orthopaedics
David R. Wilson
University of British Columbia Department of Orthopaedics, Centre for Hip Health and Mobility

Technical advance

Keywords: Standing MRI, contact area, tibiofemoral joint, knee, anterior cruciate ligament, reliability

Posted Date: January 31st, 2020

DOI: https://doi.org/10.21203/rs.2.22418/v1

Version of Record: A version of this preprint was published on November 30th, 2020. See the published version at https://doi.org/10.1186/s12891-020-03786-1.

Abstract

Background: Biomechanical studies are often performed using conventional closed-bore MR, which has necessitated simulating weightbearing load on the joint. The clinical applicability of these biomechanical findings is unclear because of the limitations of simulating weightbearing. Upright, open MRI (UO-MRI) can be used to assess knee joint mechanics, in particular contact area and centroid location. However, it is not clear how reliably measurements of contact area and centroid location can be made in upright weightbearing postures. Methods: Manual segmentation of cartilage regions in contact was performed and centroids of those contact areas were automatically determined for the medial (MC) and lateral (LC) tibiofemoral compartments. To assess reliability, inter-rater, test-retest, and intra-rater reliability were determined by intra-class correlation (ICC 3,1), standard error of measurement (SEM), smallest detectable change with 95% confidence (SDC 95). Accuracy was assessed by using a high-resolution, 7T MRI as a reference and determined by measurement error (%). Results: Contact area and centroid location reliability (inter-rater, test-retest, and intra-rater) for sagittal scans in the MC demonstrated ICC 3,1 values from 0.95-0.99 and 0.98-0.99 respectively, and in the LC from 0.83-0.91 and 0.95-1.00 respectively. The smallest detectable change in contact area was 1.28% in the MC and 0.95% in the LC. Contact area and centroid location reliability for coronal scans in the MC demonstrated ICC 3,1 values from 0.90-0.98 and 0.98-1.00 respectively, and in the LC from 0.76-0.94 and 0.93-1.00 respectively. The smallest detectable change in contact area was 0.65% in the MC and 1.41% in the LC. Contact area segmentation was accurate to within 4.81% measurement error. Conclusions: Knee contact area and contact centroid location can be assessed in upright weightbearing MRI with good to excellent reliability and accuracy within 5%. The lower field strength used in upright, weightbearing MRI does not compromise the reliability of tibiofemoral contact area and centroid location measures.

Introduction

Magnetic resonance (MR) has been used to assess knee joint mechanics for a number of applications, including explaining how acute injury such as anterior cruciate ligament (ACL) rupture increases the risk for osteoarthritis (OA)[1–5]. Measurements made include kinematics[1,6–8] cartilage contact area, and centroid location[3,5,8–10].

Most biomechanical studies have been performed using conventional closed-bore MR, which has necessitated simulating weightbearing load on the joint. Approaches include positioning the participant supine in the scanner with an axial load applied to the foot (closed kinetic chain)[3,10,11], registering unloaded MRI-based models of cartilage to measurements of bones from loaded fluoroscopic evaluations[12,13], and MR imaging in supine before and after a knee loading activity is performed[14,15]. Open kinetic chain loading has also been used, such as applying a torque to the shank while the participant lies supine[8].

The reliability and accuracy for contact area and centroid location from studies with simulated loading have been estimated. The coefficient of variation (CV) for tibiofemoral contact area and centroid location,

which indicates the extent of variability between multiple testing sessions, has ranged between 3.1-9.0% and 0.3–3.3% respectively[3,5,8,10,13]. Determining contact area by combining MRI with biplanar radiography has shown a slightly larger standard error of measurement of 14 ± 11% in a cadaveric validation study[12].

The clinical applicability of these biomechanical findings is unclear because of the limitations of simulating weightbearing in conventional scanners. Supine scans with simulated weightbearing may not represent joint behaviour under physiologic load, because the supine position does not reproduce the effect of postural muscles on joint position. Assessments pre- and post-activity provide information about acute changes that result from activity, but not necessarily the biomechanical cartilage changes that occur during it.

Upright, open MRI (UO-MRI) addresses the limitations of simulated weightbearing in supine scanners by allowing joint imaging during weightbearing[8,9,16]. However, it is not clear how reliably measurements of contact area and centroid location can be made in upright weightbearing postures.

The aims of this study were: 1) to assess the reliability and accuracy of tibiofemoral cartilage contact area and centroid location acquired both sagitally and coronally 2) to describe the implementation of an UO-MRI protocol that permits acquisition of these measures in vivo under physiologic weight-bearing conditions.

Methods

This study was approved by the UBC Clinical Research Ethics Board (H18-01459). All participants provided informed, written consent (Appendix B).

Participants

A sample of 5 patients from a larger comparative cohort study volunteered for reliability analysis. The cohort study was a convenience sample of 18 patients with prior ACL rupture. Patients were recruited through posted notifications and targeted e-mails (Appendix A).

Inclusion criteria for the cohort study were: 1) adult participants between the ages of 18–50 years old with unilateral, isolated ACL ruptures; 2) intact cartilage and evidence of complete ACL rupture on MRI; 3) reported ACL rupture within the last 5 years and if reconstructed, done within 1 year from injury; and 4) have completed a full rehabilitation program and returned to regular sport or recreational activities.

Exclusion criteria were: 1) associated ligament rupture other than the ACL (though incomplete MCL ruptures were not excluded); 2) known knee osteoarthritis diagnosed by a physician; 3) presence of other joint disease; 4) incompletely rehabilitated injury, defined as a range of motion less than 0-130 degrees, quadriceps atrophy, or persistent mechanical symptoms; 5) individuals prohibited from undergoing MRI based on the MRI screening form (Appendix C); 6) history of fainting, or evidence of change in orthostatic

blood pressure; 7) prior or subsequent knee surgery other than diagnostic arthroscopy; 8) history of corticosteroid injection to either knee; and 9) bilateral ACL rupture or ACL re-rupture.

Demographic data from participants were collected including age, height, body mass, date of injury, time from injury to surgery (if applicable), and time from injury to study participation. Validated outcome questionnaires were administered to characterize knee symptoms: the Knee Injury and Osteoarthritis Outcome Score (KOOS)[17] and the International Knee Documentation Committee Subjective Knee Form (IKDC)[18].

Imaging

Participants were scanned standing in a 0.5T upright, open MRI (MROpen, Paramed, Genoa, Italy). All scans were done in the morning, participants were instructed not to do any impact exercise prior to scanning, and participants were seated for 30 minutes prior to scanning, during which time questionnaires were administered. Participants wore compression socks to minimize venous pooling in the lower extremities during standing scans. Participants then stood for 15 minutes prior to acquiring standing scans to ensure a cartilage deformation equilibrium had been reached. Each participant wore a chest harness suspended from an aluminum ceiling track safety-rated to 450 lbs (Handicare, Concord, ON) as a precautionary measure in case the participant fainted during upright scanning. No weight was borne through the bars or the harness. Standing scans of the ACL-injured leg were acquired with the knees in full extension, with the participant instructed to stand comfortably and distribute their weight equally between legs. Three support bars (shins, buttocks, and hands) were placed to help the participant remain still during scanning. We obtained sagittal and coronal images with a double echo steady state T2 sequence (Table 1) using a commercial 2-channel knee coil (ParaMed) suspended around the knee. The sequence was optimized to provide excellent cartilage signal quickly enough to minimize the effects of patient movement and fatigue while standing. The data was denoised by an optimized blockwise nonlocal means denoising filter[19], and the component DESS images were subsequently fit to a signal model with a global T1 estimate of 0.5[20].

Table 1
Imaging parameters used for UO-MRI scans and for the high-resolution 7T standard

	0.5T UO-MRI	7T MRI
Pulse sequence	3D DESS	2D multi-slice RARE
Repetition time (ms)	16	2200
Echo time (ms)	6	8.4
Field of view (cm)	22 × 22 × 16	6 × 6
Acquisition matrix size	256 × 256 × 38	256 × 256, 50 slices
Slice thickness (μm)	2500	35.0
Slice gap (μm)	0	0
Voxel dimensions (μm)	859 × 859 × 2500	23.4 × 23.4 × 35.0
Flip angle (°)	30	180
Bandwidth (Hz/pixel)	146.9	318.4
Total scan time (min)	3 min 30sec	28 min 10sec

Raters identified tibiofemoral contact regions by manually tracing regions with no visible separation between cartilage surfaces on each image slice using the Editor module in 3D Slicer[21] (http://www.slicer.org) in both the coronal and sagittal planes (Fig. 1.A). Raters selected voxels of cartilage that were in direct contact and did not contain any contribution from other structures (e.g. meniscus or synovial fluid). Volumes were created that represented medial and lateral contact areas, each with a known number of voxels (Fig. 1.B). We multiplied the number of voxels by their known dimensions to calculate contact areas for the medial and lateral compartments. To account for differences in size between subjects, this measurement was normalized by taking the ratio (%) of the contact area over the maximum axial cross-sectional area of the tibial plateau. The centroid location was the geometric center generated from the contact area segmentations in the medial and lateral compartments (Fig. 1.B). A validated joint coordinate system was employed to locate contact area centroids within a consistent coordinate frame[22]. Centroid location was quantified as a percentage on the tibial plateau in the medial (0%) to lateral (100%) and posterior (0%) to anterior (100%) directions to account for differences in size between participants.

Accuracy

We assessed the accuracy of contact area measurement by comparing our method in the UO-MRI to reference measurements of contact area made in a 7T MR scanner (Bruker Biospin, Ettlingen, Germany) for two cartilage preparations at two load levels. We created two cartilage contact preparations by

dissecting a bovine knee and extracting medial and lateral tibial and femoral blocks using a handsaw. The block dimensions were approximately 30 mm by 30 mm in the anteroposterior direction and mediolateral direction and were approximately 20 mm in the axial (compressive) direction. The bony side of each osteochondral block was affixed to polycarbonate tissue mounts with cyanoacrylate glue. Care was taken to extract osteochondral blocks in an orientation that approximately matched and were oriented on tissue mounts in a manner that maximized contact of the flattest part of the mating joint surfaces. The preparations were immersed in phosphate-buffered saline and positioned in an MR-compatible compression chamber such that axial compression could be applied by rotating a Delrin plunger (2 mm thread) within the capsule of the compression chamber. The samples were positioned such that opposing cartilage surfaces were touching but not compressed, and images were acquired. An axial load was then applied until cartilage compression could be visualized, and the specimen was re-scanned. The displacement of the plunger was marked on the outside of the chamber so that the process could be repeated. On completion, the load was removed and the cartilage given time to equilibrate. The process was performed first on the UO-MRI and then at the 7T MRI with imaging parameters listed in Table 1.

Statistics

Inter-rater, test-retest, and intra-rater reliability statistics were calculated for tibiofemoral contact area and centroid location. Inter-rater reliability was obtained for two raters (A. M. S. and D. J. S.) who individually segmented and calculated contact areas for each scan. Test-retest reliability was established by scanning each participant twice, with approximately one month between scans, with one rater (D. J. S.) segmenting both scans. Intra-rater reliability was obtained for one rater (A. M. S.) segmenting the contact areas for each sample 3 times, each 2 weeks apart. We calculated the intra-class correlation coefficient for fixed raters ($ICC_{3,1}$) using the methods described by Shrout and Fleiss[23], the standard error of measurement (SEM), and the smallest detectable change with 95% confidence (SDC_{95}). ICCs less than 0.5 indicated poor reliability; 0.5 to 0.75 moderate reliability; 0.75 to 0.9 good reliability; and greater than 0.9 excellent reliability. All metrics were obtained for both coronal and sagittal scans.

We assessed contact area accuracy by finding the percent difference for contact areas measured using low-resolution 0.5T UO-MRI and those measured for the same region and load using high-resolution 7T MRI from images obtained in the sagittal plane.

Results

Descriptive characteristics for the 5 participants included in the reliability analysis are reported in Table 2. There were 4 female participants and 1 male; 3 had undergone ACL reconstruction and 2 had not.

Table 2
Descriptive characteristics of participants in reliability analysis

	Mean (SD)
Age (years)	23.4 (4.2)
Time since injury (years)	2.9 (1.8)
BMI (kg/m^2)	23.3 (1.1)
IKDC Subjective Score (%)	89.1 (10.2)
KOOS (%)	95.2 (3.2)

Mean absolute contact areas were 452mm^2 (± 103) and 314mm^2 (± 41) for medial and lateral compartments, respectively. Mean normalized contact areas were 13.7% (± 2.6) and 9.7% (± 1.6) for medial and lateral compartments, respectively.

For scans acquired in the sagittal plane, contact area $ICC_{3,1}$ values (including inter-rater, test-retest, and intra-rater reliability) ranged from 0.94 to 0.99 in the medial compartment, and 0.83 to 0.91 in the lateral compartment (Table 3). From the test-retest data, contact area SDC_{95} was 1.28% in the medial compartment and 0.95% in the lateral compartment. Qualitatively, contact regions were very similar between raters (Fig. 2), and centroid location demonstrated high reliability (Table 4). SDC_{95} for medial centroid locations in the X and Y direction were 3.39% and 4.94%, respectively. SDC_{95} for lateral centroid locations in the X and Y direction were 4.41% and 3.85%, respectively.

Table 3
Contact area reliability for sagittal UO-MRI scans

	Medial Compartment		Lateral Compartment	
	$ICC_{3,1}$ (95%CI)	SEM (%)	$ICC_{3,1}$ (95%CI)	SEM (%)
Inter-Rater	0.95 (0.59–0.99)	0.39	0.83 (0.06–0.98)	0.44
Test-Retest	0.94 (0.56–0.99)	0.46	0.84 (0.10–0.98)	0.34
Intra-Rater	0.99 (0.94-1.00)	0.21	0.91 (0.64–0.99)	0.31

Table 4
Centroid location reliability for sagittal UO-MRI scans

	Medial Compartment			Lateral Compartment		
	$ICC_{3,1}$ (95%CI)	X SEM (%)	Y SEM (%)	$ICC_{3,1}$ (95%CI)	X SEM (%)	Y SEM (%)
Inter-Rater	0.99 (0.97-1.00)	0.71	1.62	0.95 (0.83–0.99)	0.95	2.81
Test-Retest	0.99 (0.95-1.00)	1.22	1.78	0.98 (0.91–0.99)	1.59	1.39
Intra-Rater	0.98 (0.95-1.00)	0.15	2.44	1.00 (0.99-1.00)	0.34	0.57

For scans acquired in the coronal plane, contact area $ICC_{3,1}$ (including inter-rater, test-retest, and intra-rater reliability) ranged from 0.90 to 0.97 in the medial compartment and 0.76 to 0.94 in the lateral compartment (Table 5). From the test-retest data, SDC_{95} was 0.65% in the medial compartment and 1.41% in the lateral compartment. Again, centroid location demonstrated high reliability (Table 6). SDC_{95} for medial centroid locations in the X and Y direction were 4.04% and 6.22%, respectively. SDC_{95} for lateral centroid locations in the X and Y direction were 3.38% and 9.83%, respectively.

Table 5
Contact area reliability for coronal UO-MRI scans

	Medial Compartment		Lateral Compartment	
	$ICC_{3,1}$ (95%CI)	SEM (%)	$ICC_{3,1}$ (95%CI)	SEM (%)
Inter-Rater	0.90 (0.35–0.99)	0.54	0.87 (0.19–0.99)	0.34
Test-Retest	0.98 (0.86-1.00)	0.23	0.76 (-0.14-0.97)	0.51
Intra-Rater	0.97 (0.85-1.00)	0.35	0.94 (0.74–0.99)	0.23

Table 6
Centroid location reliability for coronal UO-MRI scans

	Medial Compartment			Lateral Compartment		
	$ICC_{3,1}$ (95%CI)	X SEM (%)	Y SEM (%)	$ICC_{3,1}$ (95%CI)	X SEM (%)	Y SEM (%)
Inter-Rater	0.99 (0.98-1.00)	0.29	1.50	0.99 (0.95-1.00	0.71	1.43
Test-Retest	0.98 (0.92–0.99)	1.46	2.24	0.93 (0.74–0.98)	1.22	3.55
Intra-Rater	1.00 (1.00–1.00)	0.27	0.54	1.00 (0.99-1.00)	0.23	0.66

In the accuracy analysis, data from one sample was discarded due to a technical error. The remaining areas obtained in the 0.5T UO-MRI for the lateral compartment unloaded, medial compartment loaded, and lateral compartment loaded were: 120mm^2, 271mm^2, and 254mm^2 respectively; areas measured using the 7T MRI were 126mm^2, 258mm^2, and 240mm^2 respectively. This produced a mean measurement error of 4.8%.

Discussion

We assessed in vivo inter-rater, test-retest, and intra-rater reliability of tibiofemoral contact area and centroid location measurements for UO-MRI scans in both sagittal and coronal planes. We evaluated the accuracy of our contact area measurements by comparing measurements made using the UO-MRI to measurements made in a high resolution 7T MRI for a bovine knee model. All measures of contact area reliability, including inter-rater, test-retest, and intra-rater, ranged from good to excellent for coronal and sagittal scans. Qualitatively, there was close correspondence between contact regions identified by different readers (Fig. 2). The accuracy analysis found an overall mean error of 4.8% between areas found from 7T MRI and from the UO-MRI. Our results suggest that sagittal or coronal scans are similarly well-suited to evaluate cartilage contact and centroid location in the tibiofemoral joint, with slightly higher repeatability values resulting from sagittal plane acquisition and evaluation.

Our assessment of SDC_{95}, the smallest amount of change that provides 95% confidence that a true change has occurred and is not due to inherent measurement error, may provide useful information for planning research studies that compliments the more widely-used ICC values. For example, our finding of SDC_{95} of 3–5% for changes in contact location (using sagittal plane images) suggests that changes in the anteroposterior direction larger than 2.5 mm can be detected (based on a 50 mm tibial plateau) using this method. This is smaller than the 4.2 mm difference reported between knees with ACL rupture and healthy knees estimated using a biplanar radiography/MRI image registration approach[24], which

suggests that our UO-MRI approach can effectively detect differences in centroid location due to ACL deficiency.

Our measures of contact area and centroid location reliability in weightbearing MR are comparable to those from 3T conventional closed-bore scans despite using a lower resolution scanner. For inter-rater reliability, our findings for contact area ICC in the medial compartment of 0.95 and in the lateral compartment of 0.83 are consistent with findings in 3T MRI of 0.90 medially and 0.92 laterally[25]. The inter-rater contact location ICCs (0.99 medially and 0.95 laterally) were also similar those found in 3T (0.99 medially and 0.91 laterally)[25]. For intra-rater reliability our findings for contact area ICC were 0.99 medially and 0.91 laterally, which was again consistent with 3T MRI findings of 0.97 both medially and laterally[25]. Our intra-rater contact location ICCs (0.99 medially and 0.98 laterally) were similar to those found in 3T (1.00 medially and 0.91 laterally)[25]. No previous study has evaluated the test-retest reliability of contact area and centroid location in vivo, although one cadaveric study examined the patellofemoral joint using a 1.5T magnet and found a test-retest ICC value of 0.98, which is comparable to our results[26]. The slightly higher variation in test-retest reliability in the current study is likely due to slight differences in participant posture and positioning between test dates, which may be easier to control in a cadaveric study. The test-retest reliability measures will be of value in experimental design, especially for studies requiring testing on more than one day. Our accuracy results, which found a mean error of 4.8%, suggest higher accuracy for our method than the results from a cadaver study using a silicone casting technique reference standard, which found a standard error of measurement of 14%[12]. This may be due to the substantial differences in the reference method for assessing contact area between the two studies.

The primary strength of this study is that it provides a comprehensive assessment of the role of the intra- and inter-individual differences in raters, and repeated scans, on the reliability of tibiofemoral contact measures. The good to excellent reliability results are supported by a large number of data sets and the inclusion of an accuracy assessment. Incorporation of both sagittal and coronal plane assessment and reporting of SDC_{95} may be useful in protocol development for future studies. Given the clear advantages for ecological validity with the UO-MRI approach for these assessments compared to traditional supine MRI, we feel that our findings have important implications for the study of knee joint mechanics and function.

The findings should be considered in light of some limitations. First, reliability was assessed in ACL-ruptured knees only. The cartilage of these participants may not be representative of cartilage in un-injured knee joints. The effect of this limitation may be that our study underestimated the reliability of our methods, because cartilage contact in healthy knee joints may be easier to identify and segment. Second, the number of samples used in the accuracy assessment was low and the reference method (7T MRI) did not represent a completely independent measure of contact area. We chose 7T MRI as it was the highest resolution possible with which we could ensure similar loads by using the same loading rig. The lengthy scan time and cost of the 7T scanner hindered our ability to process more samples for accuracy assessment; similarly, we were not able to establish the reliability of measuring contact area in the 7T

MRI before we used it as the reference standard. Third, our study was limited to two readers, and further assessment might be required for an application where a large number of readers would be involved.

Conclusions

In conclusion, knee contact area and contact centroid location can be assessed in upright weightbearing MRI with good to excellent reliability and accuracy within 5%. The lower field strength used in upright, weightbearing MRI does not compromise the reliability of tibiofemoral contact area and centroid location measures.

List Of Abbreviations

Upright, Open MRI: UO-MRI; Medial tibiofemoral compartment: MC; Lateral tibiofemoral compartment: LC; Intra-class correlation: $ICC_{3,1}$; Standard error of measurement: SEM; Smallest detectable change with 95% confidence: SDC_{95}; Magnetic resonance: MR; Anterior cruciate ligament: ACL; Osteoarthritis: OA; Coefficient of variation: CV; Knee Injury and Osteoarthritis Outcome Score: KOOS; International Knee Documentation Committee Subjective Knee Form: IKDC; Standard deviation: SD; Body mass index: BMI

Declarations

Ethics approval and Consent to Participate: This study was approved by the UBC Clinical Research Ethics Board (H18-01459). All participants provided informed, written consent (Appendix B).

Consent for Publication: Not applicable.

Availability of Data and Materials: The datasets generated and/or analysed during the current study are not publicly available as ethics approval for public dissemination of raw data was not granted but are available from the corresponding author on reasonable request.

Competing Interests: The authors declare that they have no competing interests.

Funding: This study was supported by Canadian Institutes of Health Research Project Grant #148828 (DRW), the Natural Sciences and Engineering Research Council of Canada (MAH), a Canadian Institutes of Health Research Canada Graduate Student - Master's award (DJS), the Canadian Orthopaedic Foundation Cy Frank Award (DJS, BAM, & DRW), and the UBC Clinician Investigator Program (DJS).

Authors' Contributions: AMS collected accuracy data, wrote the Introduction and Discussion of the manuscript, and edited all sections of the manuscript. DJS planned the study, collected and analyzed the data, wrote the Methods and Results of the manuscript, and edited all sections of the manuscript. AY implemented the T2 MRI sequence. BAM edited the methods section. MAH edited the methods section. DRW was the senior author and was involved with study planning and manuscript drafting. All authors read and approved the final manuscript.

Acknowledgments: The research team thanks MRI technologists Jennifer Patterson and James Zhang, advanced imaging specialist Honglin Zhang, statistician Karey Schumansky, and all of the participants.

References

1. Chaudhari AM, Briant PL, Bevill SL, Koo S, Andriacchi TP. Knee kinematics, cartilage morphology, and osteoarthritis after ACL injury. Med Sci Sports Exerc. 2008 Feb;40(2):215-22.
2. Li G, Moses JM, Papannagari R, Pathare NP, DeFrate LE, Gill TJ. Anterior cruciate ligament deficiency alters the in vivo motion of the tibiofemoral cartilage contact points in both the anteroposterior and mediolateral directions. J Bone Joint Surg Am. 2006 Aug;88(8):1826-34.
3. Chen E, Amano K, Pedoia V, Souza RB, Ma CB, Li X. Longitudinal analysis of tibiofemoral cartilage contact area and position in ACL reconstructed patients. J Orthop Res. 2018 Oct;36(10):2718-27.
4. Amin S, Guermazi A, Lavalley MP, Niu J, Clancy M, Hunter DJ, et al. Complete anterior cruciate ligament tear and the risk for cartilage loss and progression of symptoms in men and women with knee osteoarthritis. Osteoarthritis Cartilage. 2008 Aug;16(8):897-902.
5. Shin CS, Carpenter RD, Majumdar S, Ma CB. Three-dimensional in vivo patellofemoral kinematics and contact area of anterior cruciate ligament-deficient and -reconstructed subjects using magnetic resonance imaging. Arthroscopy. 2009 Nov;25(11):1214-23.
6. Defrate LE, Papannagari R, Gill TJ, Moses JM, Pathare NP, Li G. The 6 degrees of freedom kinematics of the knee after anterior cruciate ligament deficiency: An in vivo imaging analysis. Am J Sports Med. 2006 Aug;34(8):1240-6.
7. Stergiou N, Ristanis S, Moraiti C, Georgoulis AD. Tibial rotation in anterior cruciate ligament (ACL)-deficient and ACL-reconstructed knees: A theoretical proposition for the development of osteoarthritis. Sports Med. 2007;37(7):601-13.
8. von Eisenhart-Rothe R, Siebert M, Bringmann C, Vogl T, Englmeier KH, Graichen H. A new in vivo technique for determination of 3D kinematics and contact areas of the patello-femoral and tibio-femoral joint. J Biomech. 2004 Jun;37(6):927-34.
9. McWalter EJ, O'Kane CM, Fitzpatrick DP, Wilson DR. Validation of an MRI-based method to assess patellofemoral joint contact areas in loaded knee flexion in vivo. J Magn Reson Imaging. 2014 Apr;39(4):978-87.
10. Shin CS, Souza RB, Kumar D, Link TM, Wyman BT, Majumdar S. In vivo tibiofemoral cartilage-to-cartilage contact area of females with medial osteoarthritis under acute loading using MRI. J Magn Reson Imaging. 2011 Dec;34(6):1405-13.
11. Chan DD, Cai L, Butz KD, Trippel SB, Nauman EA, Neu CP. In vivo articular cartilage deformation: Noninvasive quantification of intratissue strain during joint contact in the human knee. Sci Rep. 2016 Jan 11;6:19220.
12. Bingham JT, Papannagari R, Van de Velde SK, Gross C, Gill TJ, Felson DT, et al. In vivo cartilage contact deformation in the healthy human tibiofemoral joint. Rheumatology (Oxford). 2008

Nov;47(11):1622-7.

13. Liu F, Kozanek M, Hosseini A, Van de Velde SK, Gill TJ, Rubash HE, et al. In vivo tibiofemoral cartilage deformation during the stance phase of gait. J Biomech. 2010 Mar 3;43(4):658-65.
14. Lad NK, Liu B, Ganapathy PK, Utturkar GM, Sutter EG, Moorman CT, 3rd, et al. Effect of normal gait on in vivo tibiofemoral cartilage strains. J Biomech. 2016 Sep 6;49(13):2870-6.
15. Sutter EG, Widmyer MR, Utturkar GM, Spritzer CE, Garrett WE, Jr., DeFrate LE. In vivo measurement of localized tibiofemoral cartilage strains in response to dynamic activity. Am J Sports Med. 2015 Feb;43(2):370-6.
16. Gold GE, Besier TF, Draper CE, Asakawa DS, Delp SL, Beaupre GS. Weight-bearing MRI of patellofemoral joint cartilage contact area. J Magn Reson Imaging. 2004 Sep;20(3):526-30.
17. Roos EM, Roos HP, Lohmander LS, Ekdahl C, Beynnon BD. Knee Injury and Osteoarthritis Outcome Score (KOOS): Development of a self-administered outcome measure. J Orthop Sports Phys Ther. 1998 Aug;28(2):88-96.
18. Irrgang JJ, Anderson AF, Boland AL, Harner CD, Kurosaka M, Neyret P, et al. Development and validation of the International Knee Documentation Committee Subjective Knee Form. Am J Sports Med. 2001 Sep-Oct;29(5):600-13.
19. Coupe P, Yger P, Prima S, Hellier P, Kervrann C, Barillot C. An optimized blockwise nonlocal means denoising filter for 3-D magnetic resonance images. IEEE Trans Med Imaging. 2008 Apr;27(4):425–41.
20. Heule R, Ganter C, Bieri O. Rapid estimation of cartilage T2 with reduced T1 sensitivity using double echo steady state imaging. Magn Reson Med. 2014 Mar;71(3):1137–43.
21. Fedorov A, Beichel R, Kalpathy-Cramer J, Finet J, Fillion-Robin JC, Pujol S, et al. 3D Slicer as an image computing platform for the Quantitative Imaging Network. Magn Reson Imaging. 2012;30(9):1323-41.
22. Grood ES, Suntay WJ. A joint coordinate system for the clinical description of three-dimensional motions: Application to the knee. J Biomech Eng. 1983;105(2):136-44.
23. Shrout PE, Fleiss JL. Intraclass correlations: Uses in assessing rater reliability. Psychol Bull. 1979;86(2):420-8.
24. Li G, Moses JM, Papannagari R, Pathare NP, DeFrate LE, Gill TJ. Anterior cruciate ligament deficiency alters the in vivo motion of the tibiofemoral cartilage contact points in both the anteroposterior and mediolateral directions. J Bone Jt Surg - Ser A. 2006;88(8).
25. Chen E, Amano K, Pedoia V, Souza RB, Ma CB, Li X. Longitudinal analysis of tibiofemoral cartilage contact area and position in ACL reconstructed patients. J Orthop Res. 2018;36(10).
26. Brechter JH, Powers CM, Terk MR, Ward SR, Lee TQ. Quantification of patellofemoral joint contact area using magnetic resonance imaging. Magn Reson Imaging. 2003;21(9):955–9.

Figures

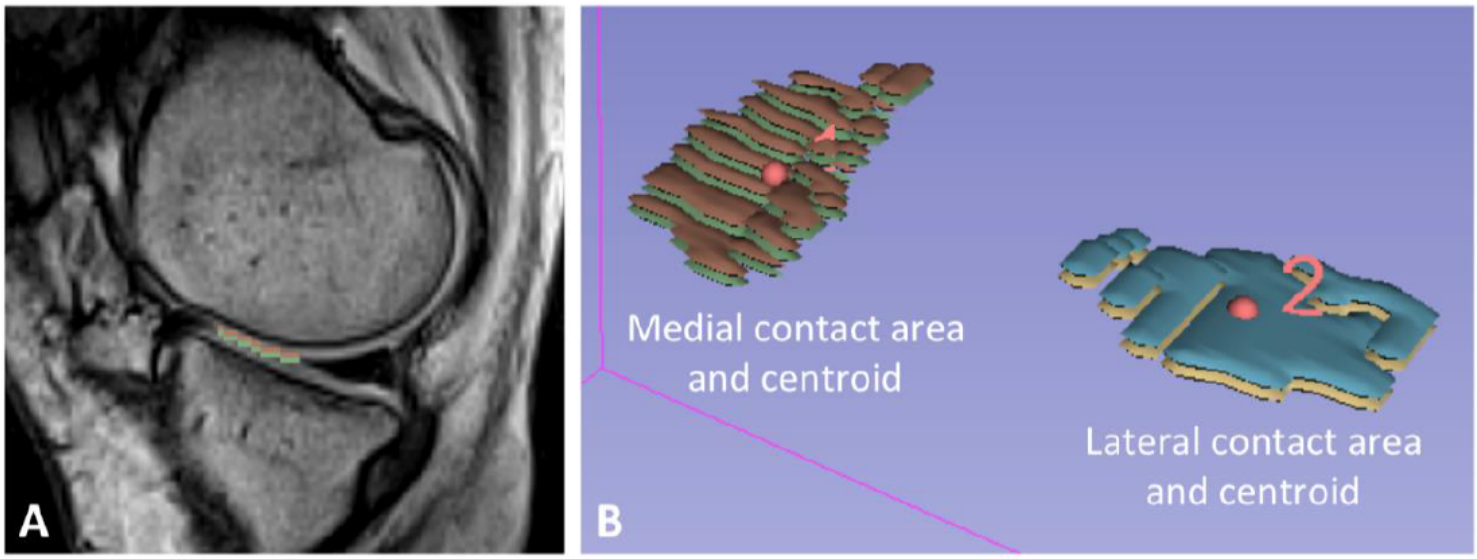

Figure 1

A) Representative sagittal slice from the medial compartment of a participant showing the tibial cartilage contact (green) and the femoral cartilage in contact (brown). B) Representative volumes of medial and lateral contact areas and contact centroids.

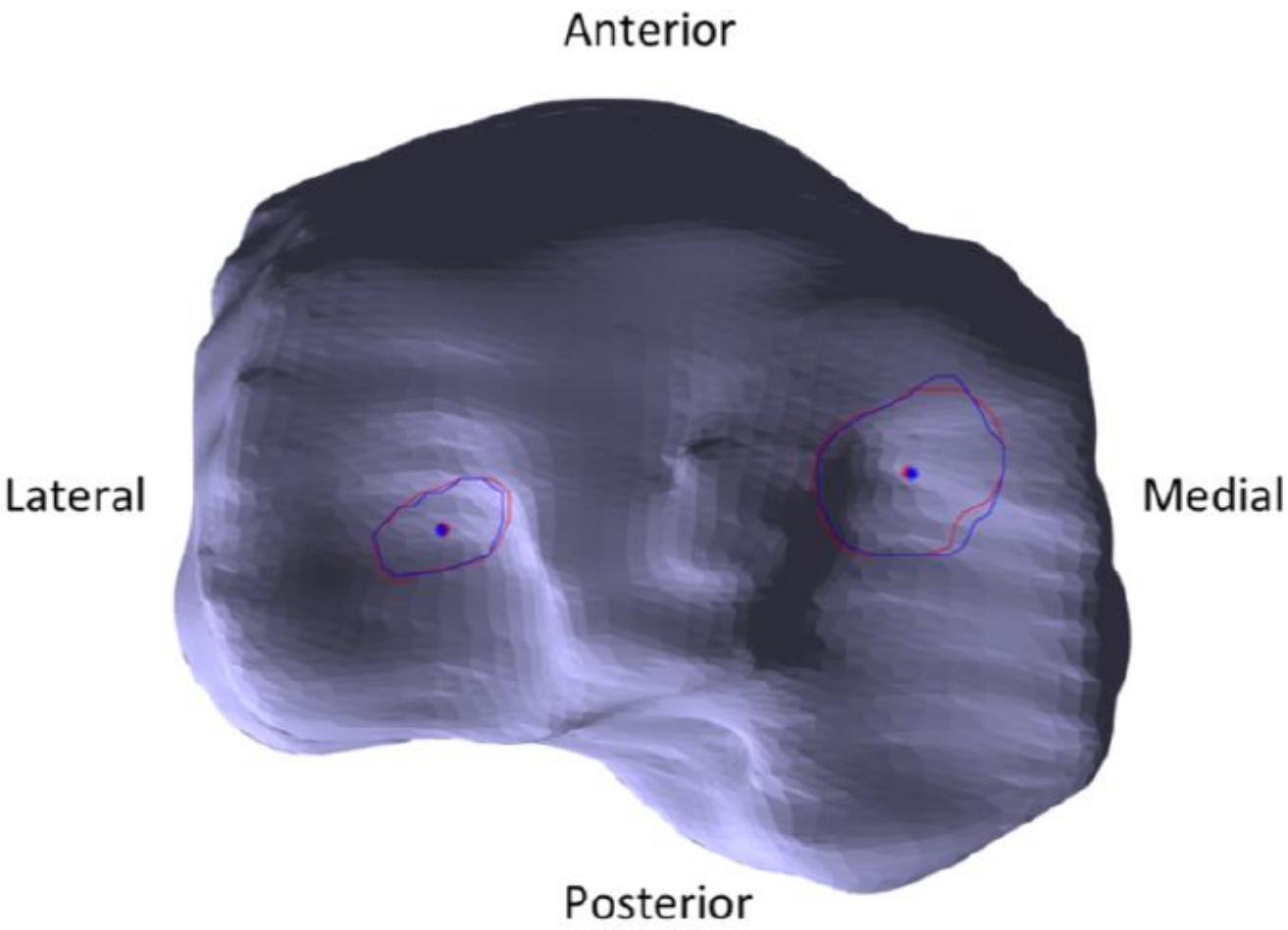

Figure 2

Axial view of a standardized tibial plateau with representative cartilage contact areas and centroid locations. Rater one cartilage contact area and centroids are in red and rater two cartilage contact area and centroids are in blue.